

## DYNAMIC EFFECTS OF ACOUSTIC RADIATION FORCE ON MICROBUBBLES

Piero TORTOLI<sup>1</sup>, Vittorio MICHELASSI<sup>2</sup>, Francesco GUIDI<sup>1</sup>, Massimo CORSI<sup>1</sup>  
Masatsugu HORI<sup>3</sup>, Ken ISHIHARA<sup>4</sup>, Fuminori MORIYASU<sup>5</sup>, Yasuhito TAKEUCHI<sup>6</sup>

The sonodynamic behaviors of compressible, encapsulated microbubbles used for ultrasonic contrast agent is known to be majorly influenced by the irradiating ultrasound field, where a few hundreds or more KPa instantaneous pressure could cause aspiration in size and shape, crushing and dissolution, displacement and flow, etc. A drastic change in its Doppler spectra under such condition is also known in many researches. In liquid suspension the acoustic radiation pressure is a major cause of such phenomena, where viscosity of the fluid is another key. This study investigates the phenomena by CW and PW Doppler method, with aid of computational simulation as well as real flow phantom data using two real and one mimicking contrast agent microbubbles.

**Keywords : Contrast agent, Microbubble, Radiation Force, Doppler, Viscosity**

### 1. INTRODUCTION

The movement of compressible, encapsulated microbubbles is known to be influenced by the application of an ultrasound field. Dayton et al.<sup>1</sup> have demonstrated through optical methods that Albnex® (Molecular Biosystems, San Diego, USA) bubbles are appreciably displaced toward the far wall of a tube by ultrasound radiation force. Doppler spectra shown by Tortoli et al.,<sup>2</sup> originated by Levovist® (Schering AG, Berlin, Germany) bubbles suspended in distilled water, exhibited considerable changes in bandwidth and shape when pressure amplitudes of a few hundreds kPa were used. Also this phenomenon was attributed to radiation force pushing the microbubbles away from the transducer.

The bubble motion was recently described as the result of the combined action of radiation pressure and drag force of the fluid where the bubble is suspended<sup>3</sup>. Because of their small inertia the bubbles react very rapidly to the ultrasound field and follow a flow path that may considerably deviate from the axial flow. The resulting relative velocity between bubbles and fluid

produces a drag force. When the drag force equals the ultrasound force the bubble trajectory is stabilized. The validity of the proposed model was demonstrated by following an indirect approach, where experimental PW Doppler spectra are compared with the simulated spectra.

In this paper, we discuss at which extent the phenomenon is affected by a) the transmitted ultrasound beam, b) the physical properties of the bubbles, c) the characteristics of the fluid. The results obtained with three different contrast agents are presented and compared to each other. We also show that, for a given bubble, different displacements are obtained in CW or PW conditions, even though the transmitted intensity is the same in the two modes.

### 2. FORCES ACTING ON MOVING BUBBLES

The following sections describe the two forces that simultaneously drive a microbubble suspended in a moving fluid insonified by an ultrasound beam.

#### 2.1 Radiation Force

The instantaneous primary force produced by an ultrasound field acting on a compressible spherical bubble can be evaluated following Dayton et al.<sup>1</sup>. The expression of the ultrasound force,  $F_{us}$ , results:

---

Received August 31, 2001

<sup>1</sup> Electronics and Telecommunications Department, University of Florence, <sup>2</sup> Dept. of Mechanical and Industrial Engineering, University of Roma Tre, Italy, <sup>3</sup> Osaka University School of Medicine, <sup>4</sup> Ehime University School of Medicine, <sup>5</sup> Kyoto University School of Medicine, <sup>6</sup> Kagoshima University, Department of Information and Computer Science, Japan.

$$F_{us}(\omega) = \frac{\pi P_a^2 D}{\rho_o c \omega} \cdot \frac{\delta_{tot} \omega_o / \omega}{\left[ \left( \frac{\omega_o}{\omega} \right)^2 - 1 \right]^2 + \left( \frac{\delta_{tot} \omega_o}{\omega} \right)^2} \quad (1)$$

where:

$P_a$  (local ultrasound pressure) and  $\omega$  (transmitted frequency) depend on the transmitted ultrasound beam;

$D$  (diameter),  $\omega_o$  (pulsing eigenfrequency) and  $\delta_{tot}$  (damping coefficient) depend on the physical properties of the microbubble;

$c$  (ultrasound propagation speed),  $\rho_o$  (fluid density) and the same  $\delta_{tot}$  depend on the fluid where the bubble is suspended.

### 2.1 Drag Force

The drag force is generated when a relative velocity exists between the bubble and the viscous fluid. In absence of radiation force, the bubbles move at exactly the same velocity of the fluid due to their vanishingly small mass. In presence of radiation force, the bubble is accelerated and diverted from the fluid flow path and a drag force develops. The drag force is proportional to the relative bubble-fluid velocity and increases until it equals the ultrasound force: at this stage the acceleration of the bubble tends to zero. Under the assumption of Newtonian fluid and spherical shape of the bubble, the size of which oscillates around a mean diameter  $D$ , the drag force,  $F_D$ , can be easily computed as follows<sup>4</sup>:

$$F_D = C_D \text{Re} \cdot \frac{\pi D \nu \rho_o}{8} \cdot |V_f - V_b| \quad (2)$$

where  $V_f$  and  $V_b$  are the fluid and bubble velocity, respectively, and  $\nu$  is the fluid kinematic viscosity.  $\text{Re}$  and  $C_D$  (Reynolds number and the drag coefficient respectively) are to be computed as:

$$\left. \begin{aligned} \text{Re} &= \frac{|V_f - V_b|}{\nu} \cdot D \\ C_D &= \frac{24}{\text{Re}} + \frac{6}{1 + \sqrt{\text{Re}}} + 0.4 \end{aligned} \right\} \quad (3)$$

The definition of  $C_D$  is strictly valid only for spherical bubbles and is accurate in the Reynolds number range [0-10<sup>5</sup>] under the hypothesis of steady flow conditions.

### 2.3 Balance of forces

The trajectory of the bubble can be traced by solving the vector motion equation:

$$\vec{F}_{us}(t) - \vec{F}_D(t) = m \cdot \frac{d \vec{V}_b(t)}{dt} \quad (4)$$

where  $m$  is the bubble mass, which, according to Leighton<sup>5</sup>, for low Reynolds numbers can be estimated equivalent to one half the mass of the displaced surrounding fluid. Equation (4) is decomposed into its radial and axial components, thereby producing two scalar equations that are marched in time by a simple Euler one-step method<sup>6</sup>. Due to their very small mass, the bubbles react instantly to the ultrasound field and can consequently deviate from the fluid core flow path<sup>3</sup>. An accurate knowledge of the parameters affecting both the ultrasound and drag forces of eq. (4) is crucial for the correct description of the bubble trajectory.

## 3. FACTORS AFFECTING THE BUBBLE DYNAMICS

### 3.1 Influence of the ultrasound beam characteristics

According to eq. (1) the radiation force is proportional to the squared value of the pressure,  $P_a$ , experienced by the bubble. Since the sound field spatial distribution is in general not uniform, moving bubbles are exposed to different pressure levels, depending on their instantaneous position. For example, a bubble crossing the axis of a beam will subsequently experience increasing pressures while approaching the beam axis, and decreasing pressures while receding from the beam axis. The extent to which the bubble is affected by radiation force will also depend on the beamwidth: large beams will deviate the bubble from its original path more consistently than narrow beams.

Since eq.(1) reports the radiation force that is instantaneously applied to a bubble, the transmission modality (Continuous Wave - CW, or Pulsed Wave - PW) plays an important role. In CW mode, the two forces are continuously applied to the bubble. In PW mode the bubble is subject to radiation force only when the ultrasound pulse travels over it. In the remaining part of the repetition interval, it is only subject to the drag force. Hence, even though the ultrasound intensity is the same in the two cases, different bubble trajectories have to be expected due to the non-linearity of the acting forces.

### 3.2 Influence of the bubble physical properties

As stated above, the radiation force acting on a bubble depends on its diameter, resonance frequency, and damping coefficient.

For a given contrast agent, the size distribution of the absolute volume fraction of gas contained in stabi-

lized microbubbles is usually non-flat around a value that is typically presented as the bubble median diameter,  $D_0$ . For each transmitted frequency, only those bubbles having a specific diameter actually resonate.

The relation between a bubble diameter and the corresponding resonant frequency,  $f_r$ , depends on the bubble mechanical properties. For free air bubbles, the resonant frequency can be computed by the following equation<sup>7</sup>:

$$f_r^2 = \frac{1}{(\pi D)^2} \left[ \frac{3}{\rho_o} \left( p_o + \frac{8\sigma}{3D} \right) \right] \quad (5)$$

where the fluid pressure,  $p_o$ , is assumed 100 kPa, and the surface tension,  $\sigma$ , is  $72 \times 10^{-3}$  N/m for bubbles in water. For encapsulated bubbles one should consider<sup>8</sup>:

$$f_r^2 = \frac{1}{(\pi D)^2} \left( \frac{3p_o}{\rho_o} \right) + \frac{2S_p}{m_e \pi} \quad (6)$$

where  $p_o$  is the fluid pressure,  $m_e$  is the effective mass of the bubble and  $S_p$  is the so-called shell parameter (including the shell elasticity and thickness). Equation (6) indicates that the stiffer is the bubble (i.e., the higher is its shell parameter), the higher is its resonance frequency. Conversely, for a given transmission frequency, stiffer contrast agents have larger resonant diameters. The presence of bubbles with different diameters implies a not uniquely defined resonant frequency for each contrast agent: for each possible frequency transmitted over a relatively wide range, there may be a corresponding group of bubbles whose diameter leads them to resonance. According to the second part of eq.1, these resonating bubbles experience the maximum radiation force, and are therefore those of major interest.

The damping coefficient,  $\delta_{tot}$ , including every radiation energy loss, depends on the bubble diameter, too. However, this parameter is less critical than the others, and an average value is usually acceptable. The damping coefficient becomes important especially when two contrast agents have approximately the same resonant diameter. In this case, the larger  $\delta_{tot}$ , the lower the ultrasound force.

**Table 1.** Main parameters influencing the radiation force for 3 contrast agents

	Levovist	Albunex	Toy Bubbles
Median diameter ( $D_o$ - $\mu\text{m}$ )	3	4	4
Shell Parameter ( $S_p$ - kg/s)	-	8	12
Damping coeff ( $\delta_{tot}$ )	0.2	0.65	0.45

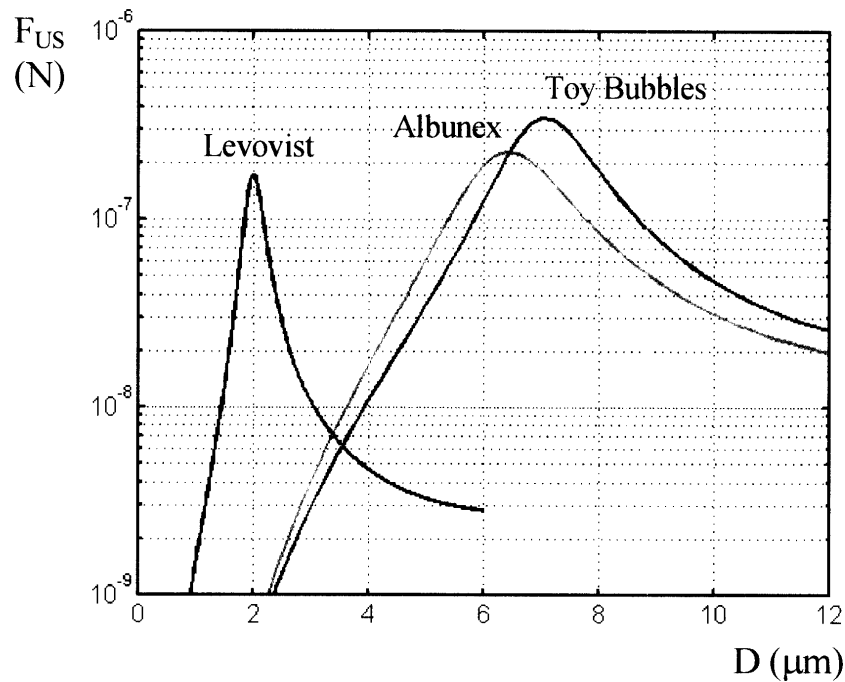


**Figure 1.** Radiation forces acting on bubbles of different diameters for 3 contrast agents suspended in distilled water ( $f = 4\text{MHz}$ ,  $P_a = 500\text{ kPa}$ )

Table 1 shows the typical values of  $D_0$ ,  $S_p$  and  $\delta_{tot}$  related to Levovist®, Albunex® and to a contrast agent mimic, F-4E® (Matsumoto Yushi-Seiyaku Co. Ltd., Osaka Japan). The latter consists of thermoplastic shell hollow microspheres containing low-molecule-number hydrocarbon gas ( $C_3H_8$ ), and will be referred here as "toy" bubbles<sup>9</sup>. In Table 1,  $S_p$  was evaluated through a method based on attenuation measurements<sup>8</sup>, while the coefficient  $\delta_{tot}$  is related to bubbles suspended in distilled water, resonating at 4 MHz. For Levovist, the shell parameter is not reported because we found that a model based on eq.(5) (free bubble) is most suitable in our case.

Fig.1 shows the radiation force evaluated for the three contrast agents as a function of the bubble diameter, when the transmission frequency is set at 4 MHz. The behavior is clearly resonant, with different resonant diameters in the three cases. In no case these are coincident with the median diameter. It may be observed that Albunex® and toy bubbles have similar resonant diameters, but radiation force is larger for toy bubbles because damping is lower.

### 3.3 Influence of the fluid characteristics

As suggested by eq. (4), equilibrium is achieved when the drag force,  $F_D$ , becomes equal to the primary ultrasound force,  $F_{us}$ . As shown in eq. (2),  $F_D$  depends on the relative velocity,  $|V_f - V_b|$ , between the fluid and the bubble, as well as on the fluid viscosity. For a given  $F_{us}$ , the  $F_D$  module that equals  $F_{us}$  requires smaller relative velocities for higher values of fluid viscosity. As an example, it has to be expected that the relative velocities reached by the bubbles due to radiation force are lower

in blood than in water, since blood kinematic viscosity is 4 times higher.

Moreover, the fluid viscosity also influences the damping coefficient. For example, for free bubbles  $\delta_{tot}$  can be considered almost proportional to  $\nu$ .

## 4. RESULTS

The combined effects of the two forces described above were simulated by considering both PW and CW transmission modalities, in the hypothesis that the bubbles initially move at constant velocity along the axis of a laminar flow. In PW mode, the radiation force is applied to the bubble only during the passage of the travelling ultrasound burst. Fig.2 shows the path followed by the resonating bubbles of 3 contrast agents when insonified by a single 5.2  $\mu$ s-long pulse directed at 45° to the fluid stream. It may be observed that, despite being subject to a lower radiation force, the Levovist bubble is radially displaced more than the others. This is consistent with the fact that the Levovist bubble resonating diameter is the lowest one, as shown in Fig.1. Hence, the other bubbles, which have larger diameters, are subject to higher drag forces that finally limit their radial displacement. In particular, the toy bubble is displaced more than the Albunex® bubble because of its minor damping.

When bubbles cross the acoustic field produced by a transducer, the entire pressure profile must be considered. Figure 3 (right) shows the total displacements imposed to a resonating Levovist bubble by 4 MHz PW and CW ultrasound fields having the pressure profile shown on the left. It may be observed that in both

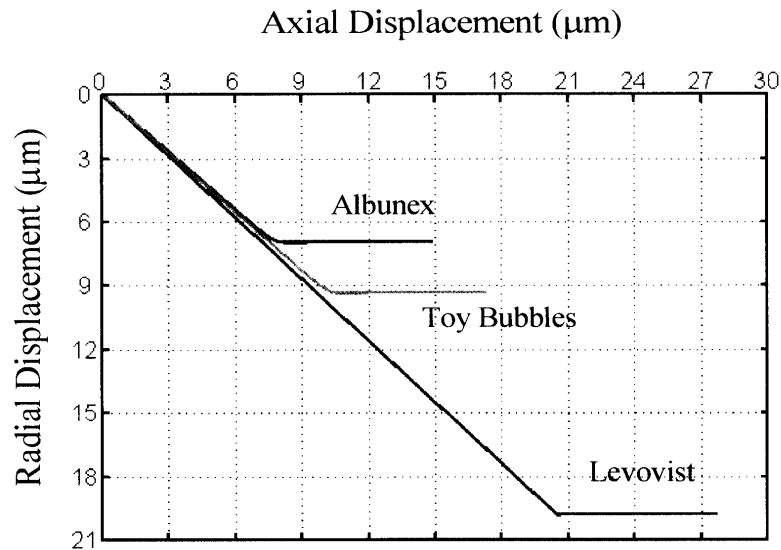


**Figure 2:** Simulated displacements of resonating Levovist, Albunex and Toy bubbles in response to a single burst of ultrasound ( $f = 4$  MHz,  $P_a = 500$  kPa)

cases the original trajectory is appreciably displaced away from the transducer in the region closer to the beam axis, where the highest pressure levels are experienced. Although the intensity is the same ( $\approx 280 \text{ mW/cm}^2$ ), the displacement is more evident in CW mode than in PW mode.

In PW mode, the estimated bubble trajectory can be used to evaluate the inter-pulse phase shifts that have to be expected between subsequent echoes backscattered from the moving bubble<sup>10</sup>. Differently from the case of scatterers moving at constant velocity (yielding constant phase shifts), here the echo-Doppler signal is typically modulated in both amplitude and phase. Its spectrum is therefore correspondingly changed, turning out to be typically asymmetrically enlarged<sup>3</sup>. Since a same contrast agent contains bubbles of different sizes, we have considered the contributions produced by a finite num-

ber of bubbles with diameters distributed over a range including the median diameter. For each bubble, the displacement due to radiation and drag force was evaluated. The individual echoes were then computed and scaled according to a factor that takes into account the size-dependent scattering cross-section<sup>8</sup>. Finally, all the echoes are summed together, to produce the simulated spectra.

An indirect demonstration of the validity of this model was achieved by comparing the Doppler spectra estimated from simulations, to those obtained from tests made with the experimental set-up described by Tortoli et al<sup>2</sup>. Fig.4 shows the simulated and experimental spectra obtained for Toy Bubbles suspended in water (left) and in a mixture of 60% water and 40% glycerol (right) at different pressure peak levels. It has to be remarked that in both cases there is an excellent agreement be-

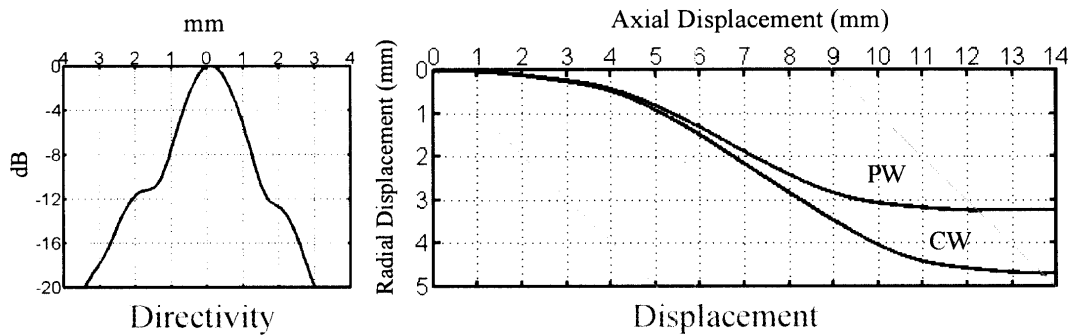


**Figure 3:** Left: pressure profile experienced by a resonant Levovist bubble suspended in a fluid moving at constant velocity ( $V_f = 12 \text{ cm/s}$ ); Right: Corresponding simulated trajectories obtained when CW and PW transmission modes are used. The beam-to-flow angle is  $45^\circ$  (i.e, it is contained within the grey oblique lines) and the ultrasound intensity is the same in the two cases

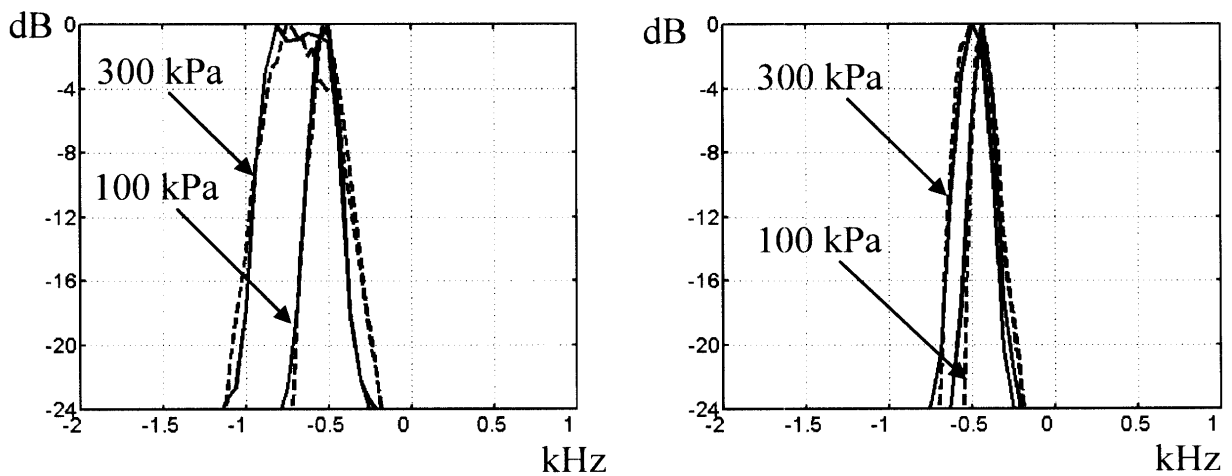


**Figure 4:** Simulated (continuous line) and experimental (dotted line) spectra obtained for Toy Bubbles suspended in water (left) and in a mixture of 60% water and 40% glycerol (right) ( $f = 4 \text{ MHz}$ ). The central streamlines of a laminar flow in a 10-mm-diameter tube were interrogated at  $45^\circ$ .

tween simulations and experiments.

## 5. DISCUSSION AND CONCLUSION

This paper has discussed the leading factors that influence the trajectory of microbubbles crossing an ultrasound field. These may be summarized in transmitted intensity, transmission modality, bubble elasticity and fluid viscosity.

Dependence on transmission intensity,  $I$ , is relatively trivial: the higher is  $I$ , the larger are the displacements. However, the comparison between displacements obtained in CW and PW modes demonstrated that the phenomenon is not linearly dependent on  $I$ , because in PW mode two distinct mechanisms are yielded, during the passage of the ultrasound pulse and during the remaining part of each pulse repetition interval, respectively.

For a given contrast agent, a different resonant diameter,  $D_{res}$ , corresponds to each possible transmission frequency. In general, the larger  $D_{res}$ , the larger the corresponding radiation and drag forces. Hence, similar displacements have to be expected<sup>3</sup>.

When different contrast agents are insonified at the same frequency, the resonant diameter depends on the bubble elasticity. The stiffer the bubble, the larger its  $D_{res}$ . Hence, the drag force is larger, too, and, unless damping reverts the situation (as for Alunex® compared to toy bubbles - see Fig.2), the bubble radial displacement is generally lower.

Finally, the fluid viscosity may drastically limit the bubble displacement. This is evident in Fig.4, which shows that the enlargement of the Doppler bandwidth is lower in a fluid having the same viscosity as blood. This fact, together with the intensity limitations imposed by FDA, may explain why the phenomenon has not been routinely reported by clinical tests.

In conclusion, there are different possible reasons yielding spectral modifications of the echoes produced by contrast agents. They are (1) resonant (harmonic) and non-resonant (chaotic) nonlinear microbubble echogenicity due to size changes, (2) echogenicity change (scintillation) appearance, growth, shrinkage and disappearance of gas bubble on and after the shell breakage, and (3) displacement of gas bubble due to transmitted ultrasound field, as discussed in this paper. The former ones typically produce repetition or symmetrical broadening of the fundamental Doppler spectrum, while the latter seems to be the only one giving rise to shifts like those visible in Fig.4.

## ACKNOWLEDGEMENTS

The authors wish to acknowledge valuable help by Alessandro Gubbini (Esaote spa, Firenze) and Emiliano Maione in the calibration of the ultrasound transducers.

## REFERENCES

1. P.A. Dayton, K.E. Morgan, A.L. Klibanov, G. Brandenburger, K.R. Nightingale and K.W. Ferrara, A preliminary evaluation of the effects of primary and secondary radiation forces on acoustic contrast agents, *IEEE Trans. on Ultrason., Ferroelect., Freq. Contr.*, 44:6, p.1264-1277 (1997).
2. P.Tortoli, F.Guidi, E.Maione, F.Curradi, V.Michellassi, Radiation force Doppler effects on contrast agents, in: *Acoustical Imaging* vol.24, H.Lee Ed., Plenum Publishing Company, New York (1999).
3. P.Tortoli, M.Pratesi and V.Michellassi, Doppler spectra from contrast agents crossing an ultrasound field, *IEEE Trans. on Ultrason., Ferroelect., Freq. Contr.*, 47:3 (2000).
4. C. Benocci, J.-M.Buchlin, V.Michellassi, P.Weinacht, Numerical modelling of gas-droplet flows for industrial applications, *Third International Conference on Computational Methods and Experimental Measurements*, Porto Carras, Greece (1986).
5. T.G. Leighton, *The Acoustic Bubble*, Academic Press, New York (1994).
6. C. Hirsch, *Numerical Computation of Internal and External Flows*, John Wiley & Sons, New York (1988).
7. B. Ran, J. Katz, The response of microscopic bubbles to sudden changes in ambient pressure, *J. Fluid Mech* 224, pp.91-115 (1991).
8. N.de Jong, *Acoustic properties of ultrasound contrast agents*, Ph.D. dissertation, de Erasmus Universiteit Rotterdam (1993).
9. Y.Takeuchi, Industrial use thermoplastic microballon to mimic the contrast agent and its in-vitro behavior including released gas dynamics, *IEEE Ultrasonics Symposium Proceed.*, pp.1579-1582 (1997).
- 10 J.A. Jensen, An analysis of pulsed wave ultrasound systems for blood velocity estimation, in: *Acoustical Imaging* vol.22, P.Tortoli & L.Masotti Eds., Plenum Publishing Co., New York, pp.377-384 (1996).